Electronic Supplementary Material (ESI) for Analyst.

Supporting information

Mimetic peroxidase based on gold amalgam for colorimetric sensing of trace mercury (II) in water samples

Jing Jiang, Xianwen Kan*

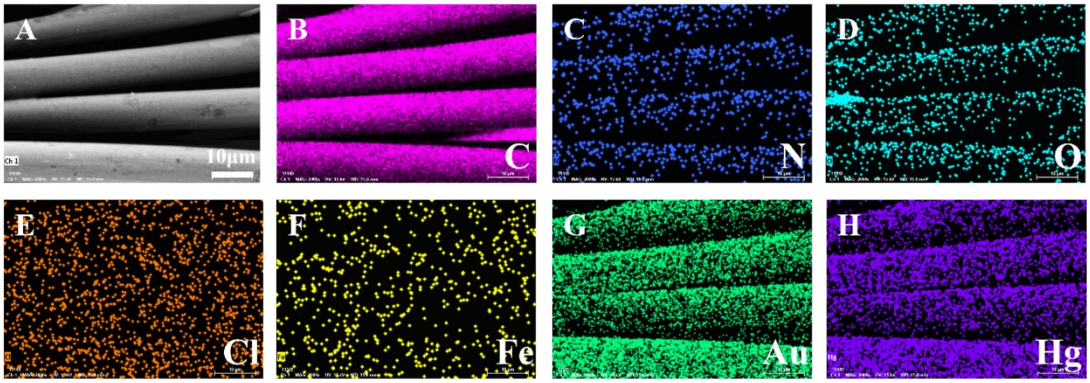

Fig. S1 Elemental mapping of Au-Hg/HrGO/CC (A-H).

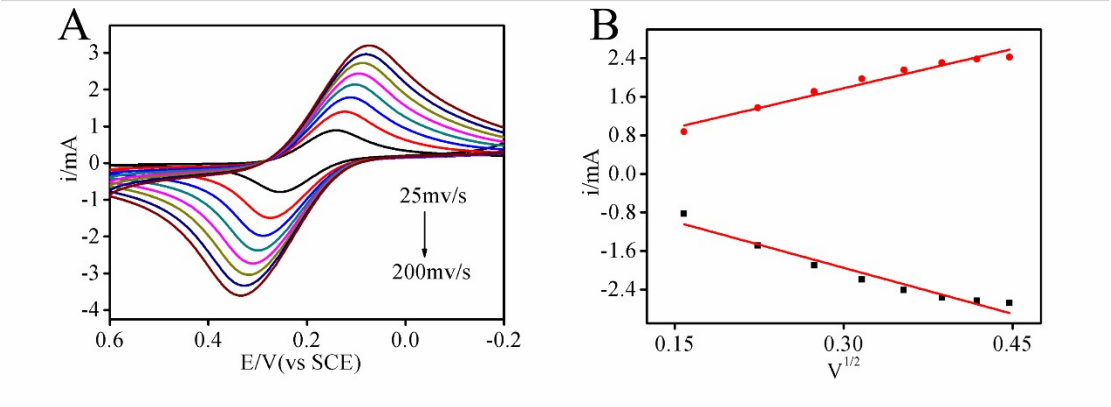

Fig. S2 CV response of AuNPs/H-rGO/CC under varieds can rates from 25 mV/s to 200 mV/s in 5.0 mM $K_3[Fe(CN)_6]$ solution. Linear fitting curve between the peak current and half power of scan rate corresponding with AuNPs/H-rGO/CC (B).

The active area of AuNPs/H-rGO/CC was measured electrochemically because conductive material CC can be used as a working electrode. The working electrode was chosen as AuNPs/H-rGO/CC with a geometric area of 0.5 cm × 0.6 cm, the reference electrode was a saturated calomel electrode (SCE), and the auxiliary electrode was a platinum electrode, respectively. CV curves were recorded on a Shanghai Chenhua CHI660C electrochemical workstation using 5.0 mM $Fe(CN)_6^{3-/4-}$ as the electrochemical probe at different scan rates (Fig. S2). The active area of AuNPs/H-rGO/CC was calculated using the Randles-Sevcik equation (equation (1)) [1,2].

$$i_p = (2.69 \times 10^5)\, n^{3/2} A D_0^{1/2} c v^{1/2} \qquad (1)$$

where i_p is the peak current intensity, n is the number of electrons transferred in the reaction (n = 1), and D_0 is the diffusion coefficient (D_0 is the ferricyanide $6.67\times10^{-6} cm^2/s$), A is the effective area of the electrode (cm^2), c is the $Fe(CN)_6^{3-/4-}$ probe concentration (mol/cm^3), and *v* is the scan rate (v/s). The effective area of AuNPs/H-

rGO/CC was calculated to be 1.84 cm^2 according to equation (1), which was approximately 6 times the geometric area. It's obvious that the high surface area of CC was beneficial to the loading of the AuNPs and H-rGO, which further facilitated to the formation of gold amalgam and the colorimetric detection of mercury ions.

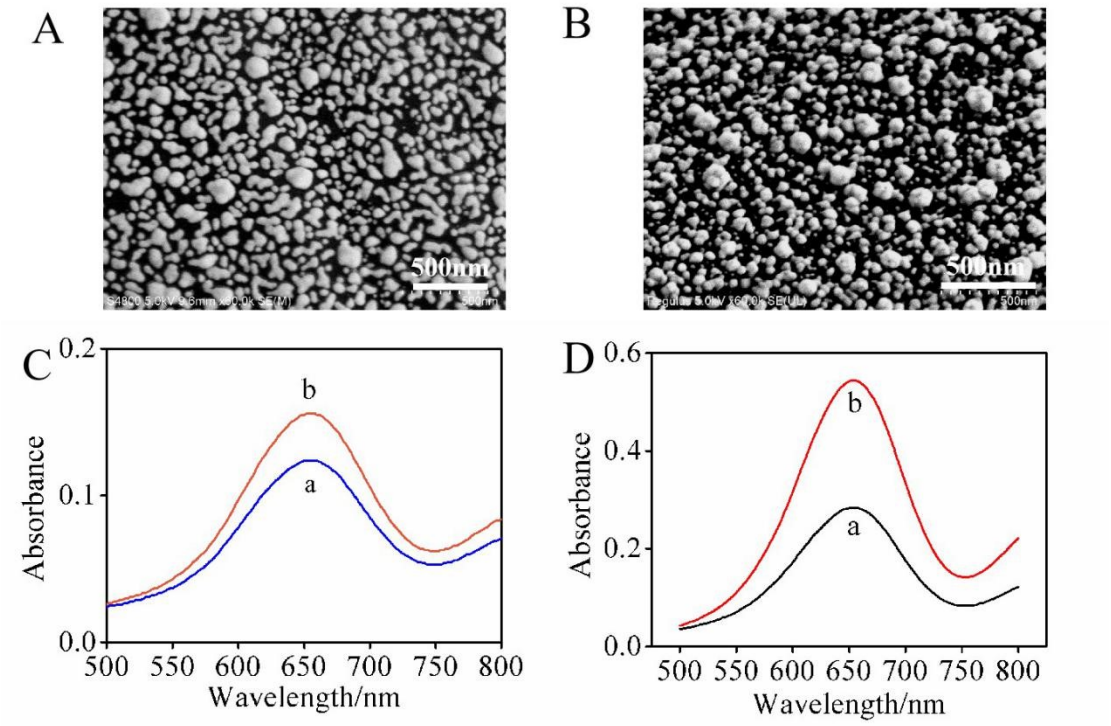

Fig. S3 SEM images of (A) AuNPs/CC at 5 polymerization turns, (B) AuNPs/H-rGO/CC at 9 polymerization circles. (C) UV spectra of AuNPs/CC before the addition of mercury (a) and after the addition of mercury (b) when the number of polymerization circles was 5. (D) UV spectra of AuNPs/H-rGO/CC before the addition of mercury (a) and after the addition of mercury (b) when the number of polymerization circles was 5.

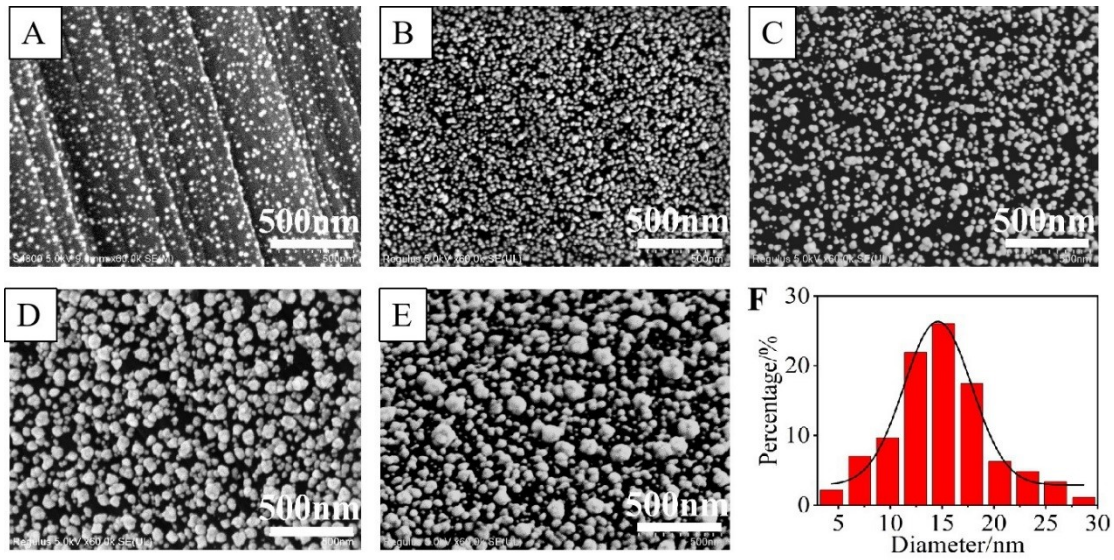

Fig. S4 SEM images of AuNPs/H-rGO/CC for Au polymerization of 1 (A), 3 (B), 5 (C), 7 (D), and 9 (E) circles, and (F) particle size distribution of AuNPs/H-rGO/CC at the optimal number of polymerization circle number.

Table S1 The comparison of the performances of different reported sensors for the determination of Hg^{2+}.

Method	Linear range (mol/L)	LOD (mol/L)	Ref.
Colorimetric	8.0×10^{-8} - 1.4×10^{-4}	1.2×10^{-9}	[3]
Colorimetric	1.0×10^{-9} - 4×10^{-7}	3.3×10^{-10}	[4]
Colorimetric	2.5×10^{-7} - 8×10^{-6}	1.6×10^{-9}	[5]
Colorimetric	1.0×10^{-6} - 5.0×10^{-6}	1.0×10^{-7}	[6]
Fluorescence	0- 6.0×10^{-5}	2.6×10^{-8}	[7]
Fluorescence	0 - 3.5×10^{-7}	1.5×10^{-8}	[8]
Fluorescence	1.0×10^{-8} - 1.5×10^{-6}	9.2×10^{-9}	[9]
Electrochemistry	3.3×10^{-7} - 3.3×10^{-6}	2.0×10^{-10}	[10]
Chemiluminescence	1.0×10^{-7} - 2.5×10^{-5}	1.0×10^{-8}	[11]
Electrochemiluminescence	1.0×10^{-8} - 5×10^{-6}	5×10^{-9}	[12]
Colorimetric	3.2×10^{-10} - 1.0×10^{-6}	3.8×10^{-10}	this work

Table S2 Determination of Hg^{2+} in different water samples.

Samples	Added (mol/L)	Found (mol/L)	Recovery (%)	RSD (%)
Tap water	1.0×10^{-7}	9.83×10^{-8}	98.25	2.21
	1.0×10^{-9}	1.0×10^{-9}	100.11	4.34
mineral water	1.0×10^{-7}	1.01×10^{-7}	100.78	1.90
	1.0×10^{-9}	1.03×10^{-9}	102.67	3.81
Lake water	1.0×10^{-7}	1.0×10^{-7}	100.13	1.10
	1.0×10^{-9}	9.82×10^{-10}	97.04	1.10
River water	1.0×10^{-7}	1.01×10^{-7}	101.42	2.18
	1.0×10^{-9}	1.01×10^{-9}	101.33	1.10
Industrial wastewater 1	1.0×10^{-7}	9.70×10^{-8}	103.03	3.32
	1.0×10^{-9}	1.03×10^{-9}	102.66	3.26
Industrial wastewater 2	1.0×10^{-7}	1.0×10^{-7}	100.16	2.89
	1.0×10^{-9}	1.0×10^{-9}	100.07	2.21

Reference

[1] T. R. L. C. Paixão, Measuring Electrochemical Surface Area of Nanomaterials versus the Randles−Ševčík Equation, ChemElectroChem, 2020,7,3414-3415.

[2] Z. Abdi, M. Vandichel, A. S. Sologubenko, M.-G. Willinger, J.-R. Shen, S. I. Allakhverdiev and M. M. Najafpour, Int. J. Hydrogen Energ., 2021, 46, 37774-37781.

[3] L. Xing, Q. Zhao, X. Zheng, M. Hui, Y. Peng, X. Zhu, L. Hu, W. Yao and Z. Yan, ACS Appl. Nano. Mater., 2021, 4, 3639-3646. DOI: 10.1021/acsanm.1c00157.

[4] W.-R. Cui, C.-R. Zhang, W. Jiang, R.-P. Liang, S.-H. Wen, D. Peng and J.-D. Qiu, ACS Sustain. Chem. Eng., 2019, 7, 9408-9415. DOI: 10.1021/acssuschemeng.9b00613.

[5] P. Ju, Z. Wang, Y. Zhang, X. Zhai, F. Jiang, C. Sun and X. Han, Colloid Surface A, 2020, 603, 125203. DOI: 10.1016/j.colsurfa.2020.125203.

[6] Y. Zhang, J. Song, Q. Pan, X. Zhang, W. Shao, X. Zhang, C. Quan and J. Li, J. Mater. Chem. B, 2020, 8, 114-124. DOI: 10.1039/c9tb02183c.

[7] S. Yu, W. Li, Y. Fujii, T. Omura and H. Minami, ACS Sustain. Chem. Eng., 2019, 7, 19157-19166. DOI: 10.1021/acssuschemeng.9b05142.

[8] S. Subedi, L. N. Neupane, H. Yu and K.-H. Lee, Sensor. Actuat. B-Chem., 2021, 338, 129814. DOI: 10.1016/j.snb.2021.129814.

[9] Y. Zhang, S. Guo, Z. Jiang, G. Mao, X. Ji and Z. He, Anal. Chem., 2018, 90, 9796-9804. DOI: 10.1021/acs.analchem.8b01574.

[10] X. Pang, H. Bai, H. Zhao, Y. Liu, F. Qin, X. Han, W. Fan and W. Shi, ACS Appl. Mater. Inter, 2021, 13, 46980-46989. DOI: 10.1021/acsami.1c10260.

[11] M. Saqib, S. Bashir, H. Li, C. Li, S. Wang and Y. Jin, Anal. Chem., 2019, 91, 12517-12524. DOI: 10.1021/acs.analchem.9b03314.

[12] Q. Zhai, H. Xing, X. Zhang, J. Li and E. Wang, Anal. Chem., 2017, 89, 7788-7794. DOI:10.1021/acs.analchem.7b01897.